

Design of a Directional Antenna Based on a Resonance Based Reflector and Its Applications on Bio-Electromagnetics

Xiao-Feng Li¹, Yan-Ru Hua¹, Bao-Jian Wen¹, Lin Peng^{1, 2, *}, and Xing Jiang¹

Abstract—A wideband resonance-based reflector (RBR) is proposed in this paper. It has an in-phase reflection band from 2.61 GHz to 5.59 GHz (72.68%), while high reflection magnitude is also obtained in the band. The proposed RBR was applied to an elliptical monopole antenna, and then, the omnidirectional radiation patterns are transformed to be unidirectional ones. The antenna profile is only 0.12λ . The proposed antenna has a measured impedance band of 2.12 GHz to 6 GHz (95.57%) and a measured front-to-back ratio band (FBR > 10 dB) of 2.2 GHz to 4.68 GHz (72.09%). The maximum FBR is up to 27.21 dB, and the antenna has good radiation performances. In addition, the proposed antenna is applied to investigate the electromagnetic characteristics of a human head. The transmission characteristics of electromagnetic wave in human head and the interactions between the human head and the electromagnetic wave were studied. The field distribution and specific absorption rate (SAR) are also discussed. Research found that the antenna matched well with the human head as good field distribution and propagation characteristics were obtained, and the antenna meets the safety standards.

1. INTRODUCTION

Broadband directional antennas have the advantages of high security, high efficiency, and strong anti-interference. They are widely used in many fields, such as ground penetrating radar [1], communication satellites, and bio-electromagnetic fields. In the field of bio-electromagnetics, they are used for the detection and imaging of human diseased tissues (such as strokes, brain tumors, and breast cancers [2]). Wideband and unidirectional radiations are required for many applications. At present, there are two main methods for obtaining directional radiation. One is that the antenna itself is an end-fire radiation antenna such as a horn antenna and a Vivaldi antenna [3]. Although horn antennas have good directivity and high gains, they have large size and heavy weight, which make them not suitable for applications where miniaturization is required. Although a Vivaldi antenna has a wide bandwidth and good directivity, it belongs to an end-fire antenna, and its profile is generally large. Another method is to load a reflector plate, such as loading a metal reflector plate, an artificial magnetic conductor (AMC), and a frequency selective surface (FSS). A metal reflector loaded directional antenna can achieve better directional performance. However, the distance between the antenna and the reflector requires $\lambda/4$ to achieve the in-phase superposition of electromagnetic waves (λ free space wavelength). Therefore, this type of antenna has a large profile and a narrow bandwidth. In recent years, with the development and application of metamaterials, the performance of antennas has been greatly improved. For example, electromagnetic bandgap (EBG) [4, 5] and AMC [6–8] can effectively reduce the cross-sectional size of the antenna and improve the radiation performance of the antenna. In addition, loading FSS [9] can also improve the directional performance and bandwidth of the antenna. However, these metasurfaces

Received 25 March 2020, Accepted 12 June 2020, Scheduled 27 June 2020

* Corresponding author: Lin Peng (penglin528@hotmail.com).

¹ Guangxi Key Laboratory of Wireless Wideband Communication and Signal Processing, Guilin University of Electronic Technology, Guilin, Guangxi 541004, China. ² School of Physics, University of Electronic Science and Technology of China, Chengdu 610054, China.

are periodic repeating structures, and multiple repeating unit structures are required to show good reflection performance, which will inevitably increase the antenna size. For example, in [9], the lateral dimension of the antenna is $1.19\lambda \times 1.19\lambda$. In addition, AMC-loaded antennas have a narrow operating frequency band.

The concept of Resonance-Based Reflector (RBR) was first proposed in [10]. The working principle of a ring-shaped resonant reflector was analyzed and studied in detail. This type of antenna has the advantages of wide frequency band, small size, and directional radiation. However, the design of a ring-shaped resonant reflector has the disadvantages of low reflection amplitude and narrow front-to-back ratio (FBR) bandwidth. The RBR antennas in the literature [11, 12] use a vertically balun feed method, which increases the profile of the antennas and limits their application in low profiles.

In this paper, a broadband resonant reflector is designed in order to solve the problems of low reflection amplitude and narrow front-to-back specific bandwidth. The in-phase reflection band of the proposed RBR is 2.6 GHz to 5.59 GHz (72.68%). The reflector is loaded into an elliptical monopole antenna to form a good directional radiation. The front-to-back ratio bandwidth (10 dB) of the antenna is 2.2 GHz to 4.68 GHz (72.09%); the highest front-to-back ratio is 27.21 dB; and the impedance bandwidth is 2.12 GHz to 6 GHz (95.57%). The height of the antenna is only 0.12λ . The antenna can be applied to a small-scale or space-constrained electromagnetic wave application environment. In this paper, the antenna is applied to the electromagnetic detection of the human head model, and the field distribution and specific absorption rate (SAR) under the human head tissue are analyzed.

2. DESIGN OF RESONANT REFLECTOR ANTENNA

The resonance based reflector can be analyzed by transmission line theory and can be equivalent to an RLC series resonant circuit [10]. Its impedance is

$$Z_L = R + j\omega L + \frac{1}{j\omega C} = R + j\frac{\omega^2 LC - 1}{\omega C} \quad (1)$$

The magnitude of the reflection coefficient $|\Gamma_L|$ and reflection phase φ_L are

$$|\Gamma_L| = \sqrt{\frac{(R - Z_0)^2 + \left(\frac{\omega^2 LC - 1}{\omega C}\right)^2}{(R + Z_0)^2 + \left(\frac{\omega^2 LC - 1}{\omega C}\right)^2}} \quad (2)$$

$$\varphi_L = \arctan\left(\frac{2Z_0 \frac{\omega^2 LC - 1}{\omega C}}{R^2 + \left(\frac{\omega^2 LC - 1}{\omega C}\right)^2 - Z_0^2}\right) \quad (3)$$

In the above, ω represents the angular frequency. R , L , and C represent the equivalent resistance, equivalent inductance, and equivalent capacitance of the resonant reflector, respectively. Z_0 represents the characteristic impedance.

If a plane wave is incident perpendicularly to the surface of the resonant reflector, Z_s represents the surface impedance of the reflector, and φ_s represents the surface phase of the reflector, then the surface phase of the resonant reflector can be expressed as

$$f_s = \text{Im}\left[\ln\left(\frac{Z_s - \eta}{Z_s + \eta}\right)\right] \quad (4)$$

where η is the wave impedance in free space.

According to Equation (4) [10], when $Z_s = 0$, $\varphi_s = \pi$, the reflecting surface is equivalent to a perfect electric conductor (PEC). When $Z_s = \infty$, $\varphi_s = 0$, the reflecting surface is equivalent to an ideal magnetic conductor (Perfect Magnetic Conductor, PMC). It can be known from Equation (1) that when the angular frequency ω is not 0, the surface impedance of the resonant reflector is a finite

value, so the reflection phase $\varphi_s \in (0, \pi)$ of the resonant reflection. The reflection phase of the resonant reflector is $0 < \varphi_s < \pi$ [10]. When it is used as an antenna reflector, the distance between the radiating unit and the reflector will be less than $\lambda/4$.

The proposed RBR in this paper is mainly composed of a large metal ring and four small metal rings whose center is located within $\pm 45^\circ$ of the large ring. The relative dielectric constant F4B of the dielectric substrate is $\epsilon_r = 2.65$, as shown in Fig. 1(a). We model and simulate the resonant reflector in the electromagnetic simulation software CST.

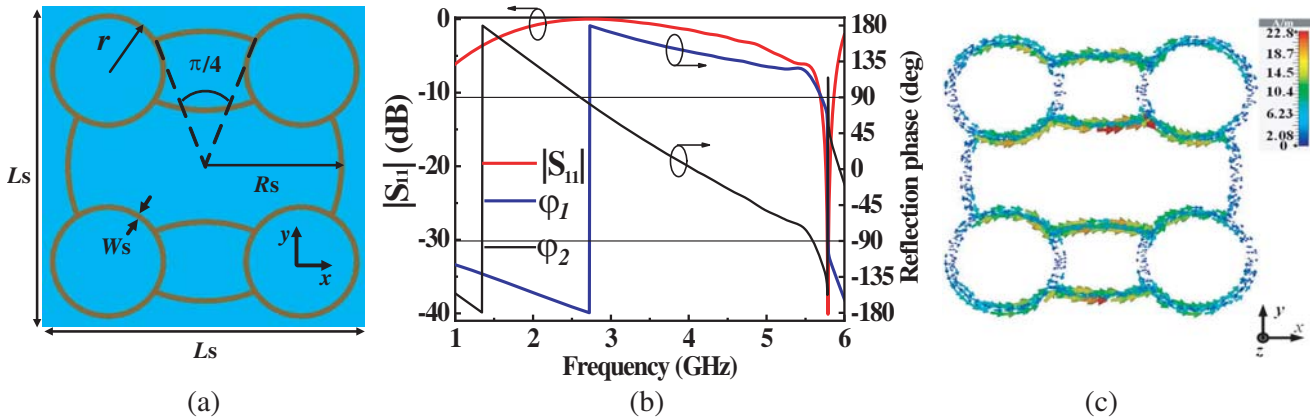


Figure 1. RBR structure diagram and simulation results. (a) structure, (b) reflection amplitude and reflection phase, (c) surface current distribution at the resonance ($r = 10$, $W_s = 1$, $L_s = 28$, $R_s = 24$, all dimensions are in millimeters).

From Fig. 1(b), the resonant frequency of the reflector is about 2.73 GHz (the frequency point where the value of $|S_{11}|$ is 0 dB). Compared with the reflector in [13], the resonance frequency is reduced by 18.51% with the same structure size. This phenomenon is because the current path of the ring resonator is longer as indicated in Fig. 1(c). In addition, the resonant reflector has a wide in-phase frequency band, and its in-phase reflection band is 2.61 GHz to 5.59 GHz (72.68%).

3. ANALYSIS OF RBR ANTENNA

The proposed RBR is applied to a monopole antenna as shown in Fig. 2. The reflector is supported by a nylon cylinder with a length $h = 18$ mm. The other parameters of the antenna are shown in the caption of Fig. 2.

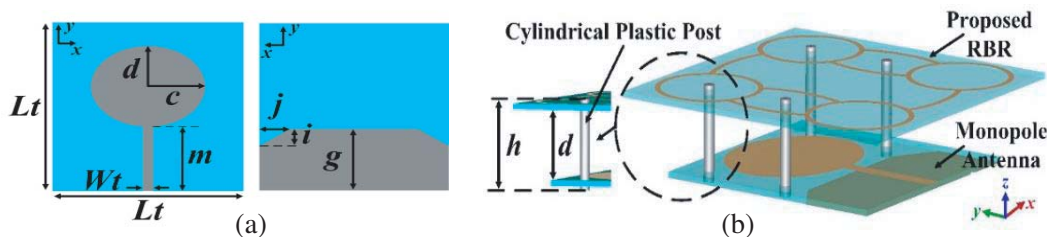


Figure 2. RBR directional antenna diagram. (a) Elliptical monopole radiation antenna Structure, (b) RBR directional antenna model diagram. ($c = 15$, $d = 14$, $g = 18.4$, $I = 5$, $j = 8$, $L = 56$, $L_t = 44$, $m = 19$, all dimensions are in millimeters).

Pictures of the fabricated antenna and measurement environment are shown in Fig. 3. The overall size of the antenna is $56 \times 56 \times 16$ mm³ ($0.43\lambda_L \times 0.43\lambda_L \times 0.12\lambda_L$; λ_L is the wavelength corresponding to the lowest working frequency of the antenna; and the instrument used for S_{11} measuring is the AV3656B

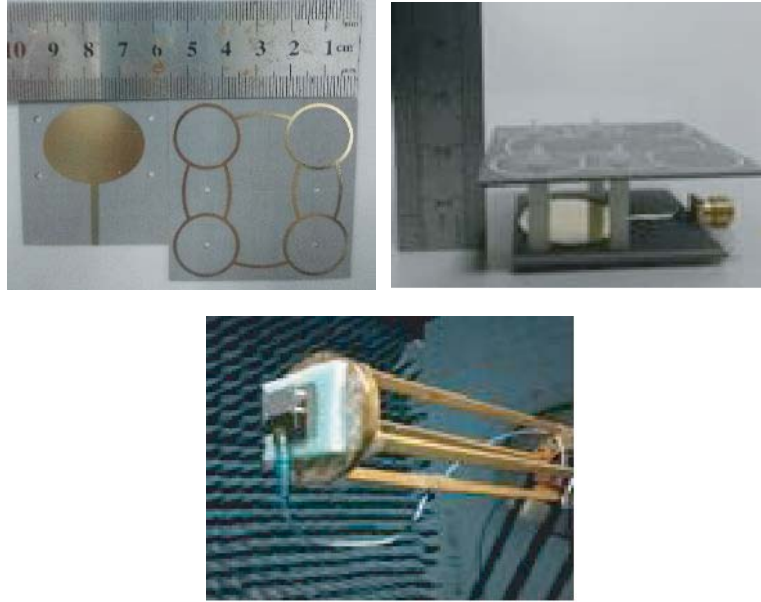


Figure 3. The fabricated antenna and the measurement environment antenna.

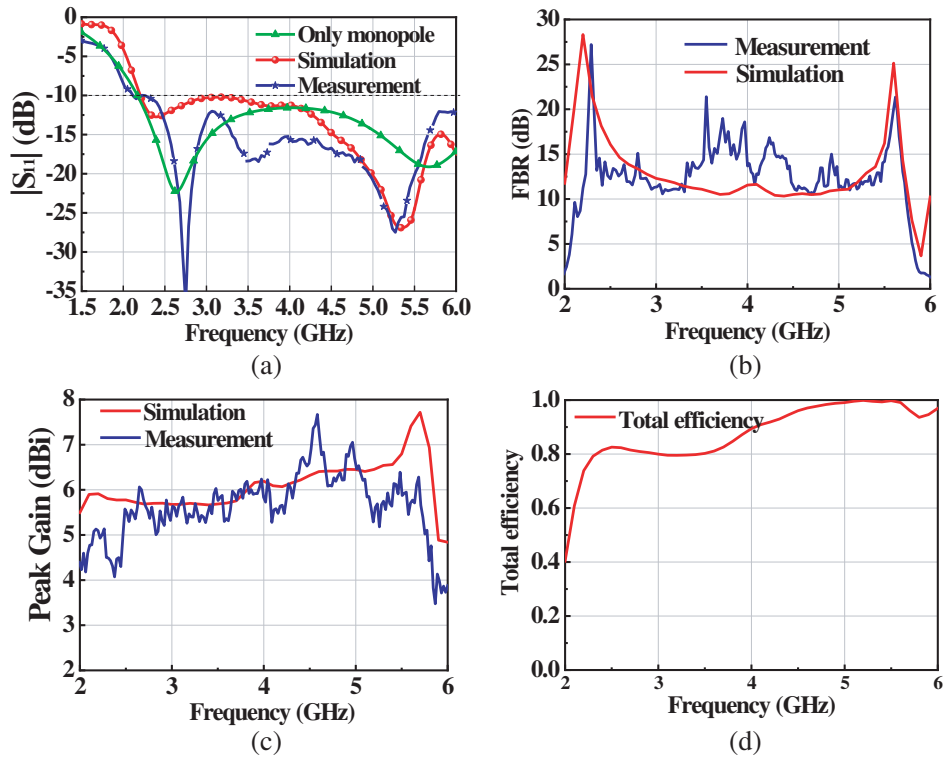


Figure 4. Results of the RBR directional antenna. (a) reflection coefficient S_{11} , (b) Front-to-back ratio FBR, (c) Gain, (d) Radiation efficiency.

vector network analyzer, pattern, etc. The radiation patterns are measured in a microwave darkroom using the NSI2000 spherical system.

The simulation and measurement results of the antennas are presented in Fig. 4. Note that the FBR and gain were measured using two identical antennas face to face. From Fig. 4(a),

the simulated impedance bandwidth is 2.20 GHz to 6 GHz (92.68%), and the measured impedance bandwidth is 2.12 GHz to 6 GHz (95.57%). From Fig. 4(b), the measured front-to-back ratio bandwidth (FBR > 10 dB) is 2.2 GHz to 4.68 GHz (72.09%), and the maximum front-to-back ratio reaches 27.21 dB. The measured and simulated gains of the antenna roughly agree with each other as shown in Fig. 4(c). The antenna radiation efficiency is greater than 80% in the entire working frequency band. The antenna has high radiation efficiency (see Fig. 4(d)).

Figure 5 shows the radiation patterns of 3 GHz, 4 GHz, and 5 GHz, which present good unidirectional radiating. Due to the limitation of the measurement system (only half of the space can be measured), the actual measurement pattern is formed by measuring the front and back parts of the antenna separately, and then combining them. However, the measured patterns still verify the simulated ones.

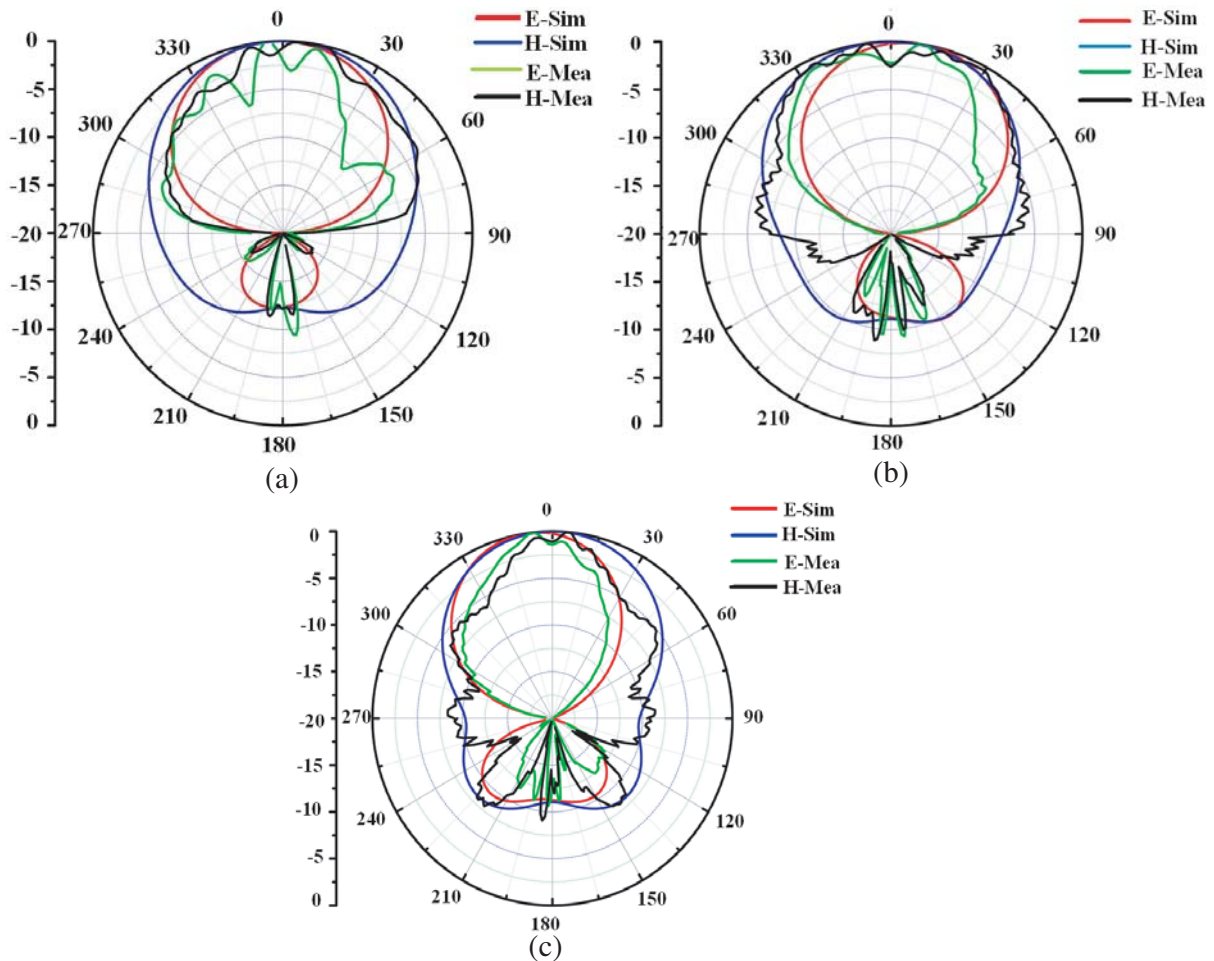


Figure 5. Radiation patterns. (a) 3 GHz, (b) 4 GHz, (c) 5 GHz.

4. CHARACTERISTIC ANALYSIS OF THE RBR ANTENNA IN MICROWAVE DETECTION OF HUMAN HEAD

4.1. Field Distribution in a Human Head with the Antenna

The RBR antenna designed is placed in different parts of the human head for simulation. The transmission of electromagnetic waves in the human head is studied, and the SAR of the antenna in the human head is analyzed.

The electric field distributions at 3 GHz, 4 GHz, 5 GHz, and 6 GHz of the human head with the antenna are presented in Fig. 6. It can be seen from the figure that the antenna can match the skull medium to form effective radiation, and the antenna has good directivity. As the frequency of electromagnetic waves increases, the electric field inside the human head will weaken, and the depth of electromagnetic waves entering the human head decreases. Therefore, it is better than the antenna that works at 3 GHz and 4 GHz.

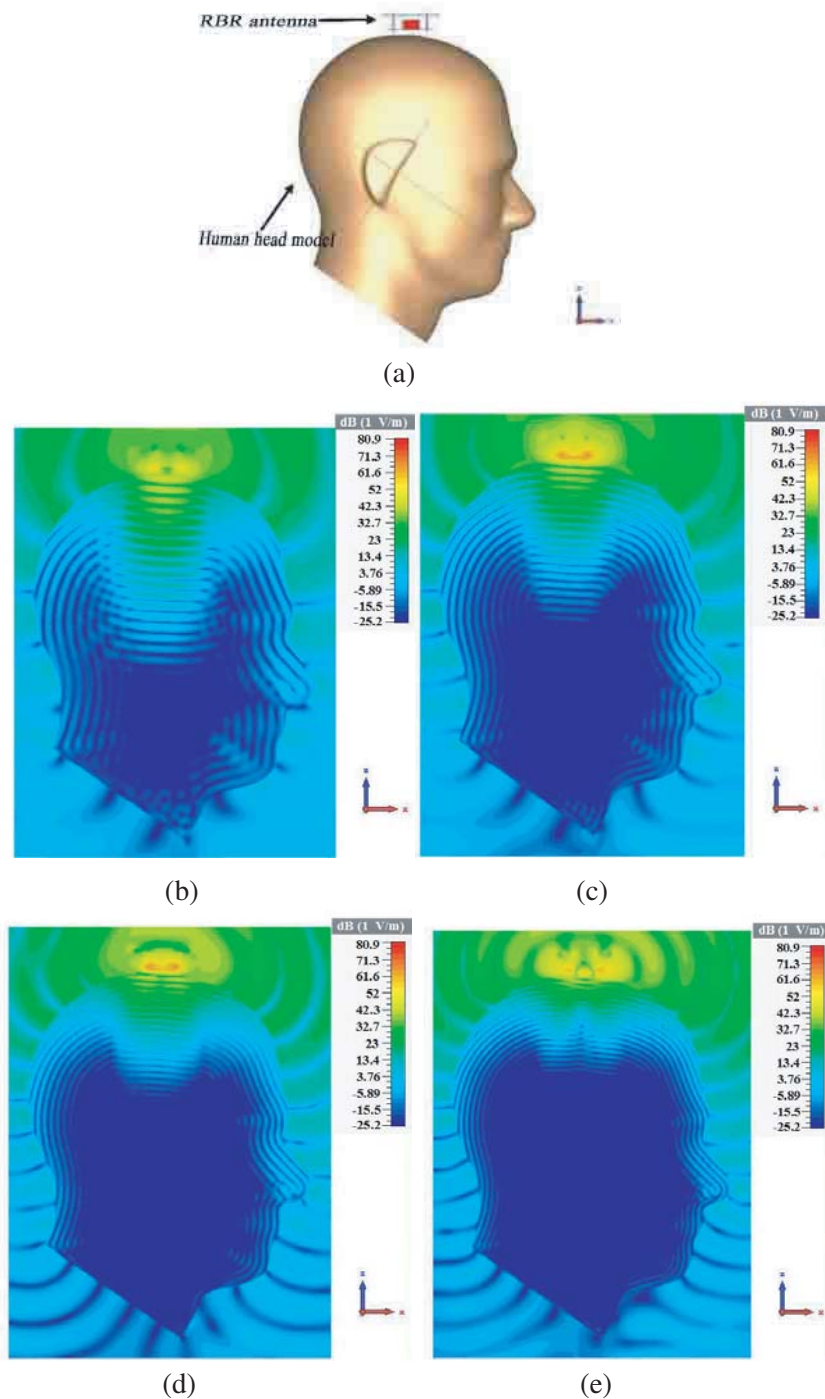


Figure 6. Electric field distribution of the antenna at different frequencies in the human head. (a) Simulation model, (b) 3 GHz, (c) 4 GHz, (d) 5 GHz, (e) 6 GHz.

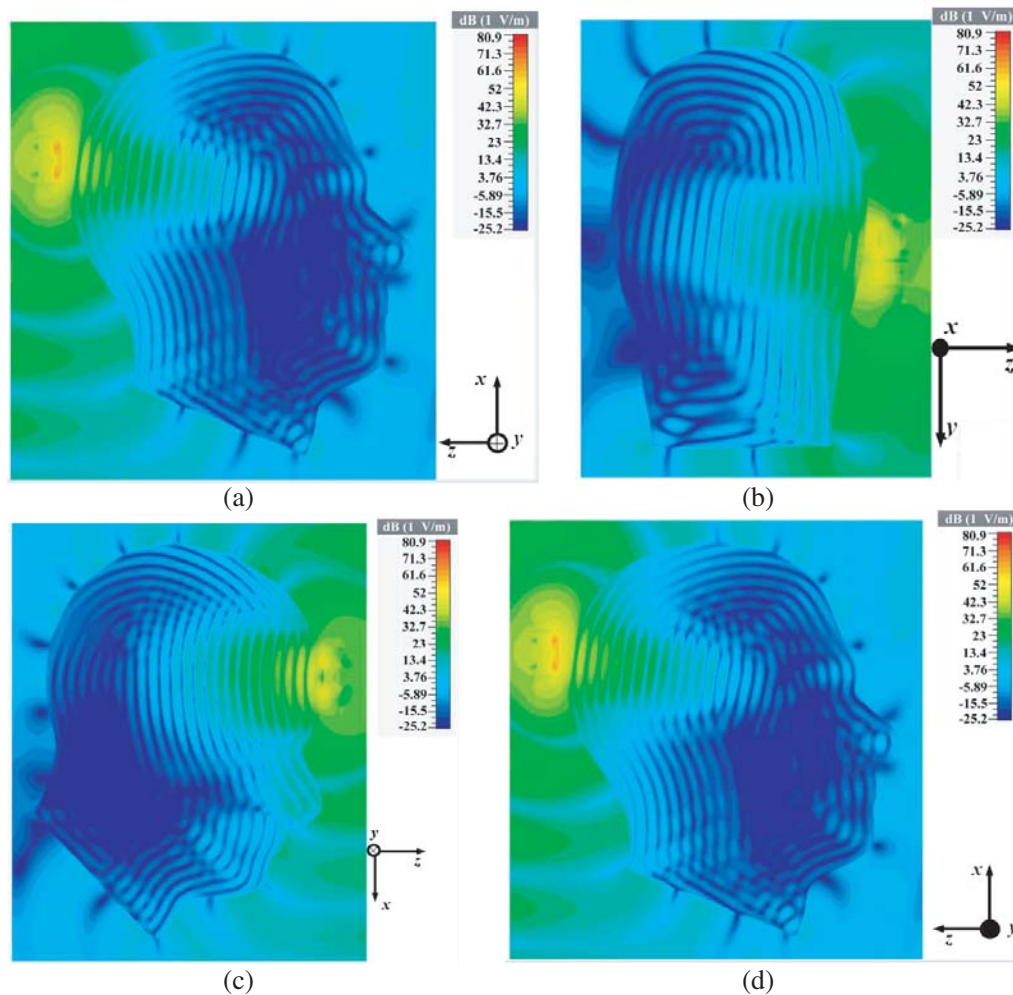


Figure 7. Simulation results of the electric field distribution of the antenna at different positions in the human head. (a) Top, (b) back, (c) forehead, (d) side.

The electric field distribution diagrams with the RBR antenna at different positions on the human head are presented in Fig. 7. It can be seen from the figure that the range of antenna electromagnetic waves transmitted from top and in front of the human head is relatively large, while the electromagnetic waves transmitted from back of the human head are attenuated. In summary, when the human head is detected, the difference in the electromagnetic characteristics of the human head structure in all directions results in different propagation characteristics at different positions.

The antenna matching characteristics with human head are studied in Fig. 8, with the S_{11} curves of the antenna at different positions of the human head. The reflection of the human head medium deteriorates the impedance matching of the antenna. However, the antenna still maintains wideband characteristics.

4.2. SAR Analysis of Resonant Reflector Antenna in Human Head Field Distribution in a Human Head with a Resonant Reflector Directional Antenna

Figure 9 shows the SAR of the antenna at different positions of the human head with an operating frequency of 3 GHz and an input power of 10 mW. The graph is the SAR value distribution at a standard of 10 g/(W/kg). It can be seen from the figure that the maximum SARs of the antenna in different parts of the human head are 0.539 W/kg, 0.931 W/kg, 1.02 W/kg, and 1.08 W/kg, which are all less than the safety standard value.

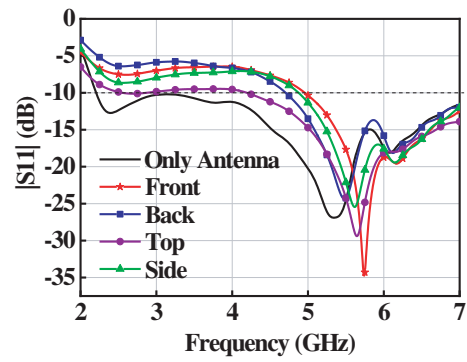


Figure 8. S_{11} of the antenna at different positions of the human head.

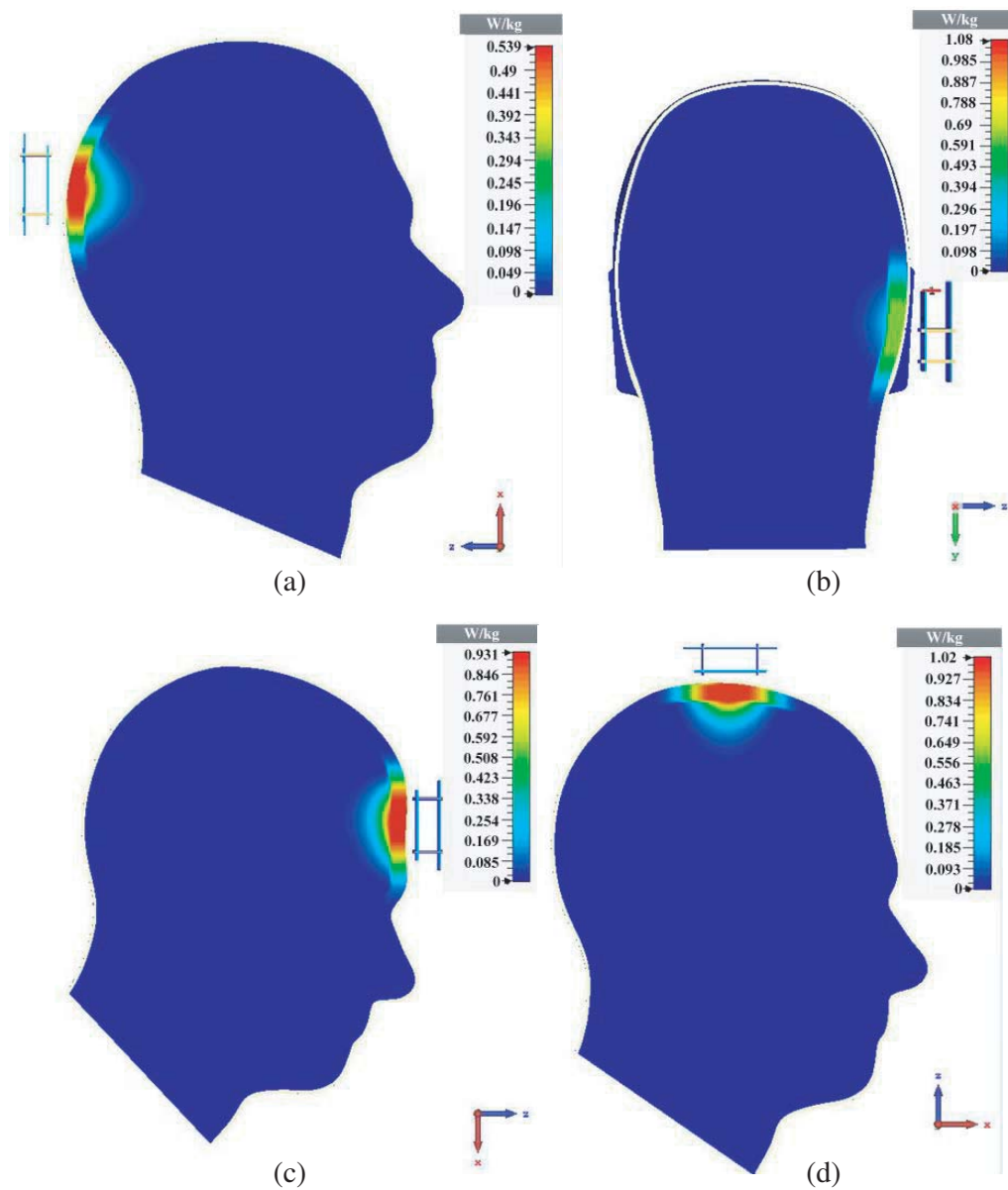


Figure 9. SAR value of the antenna when working at different positions of the human head, (a) back, (b) side, (c) forehead, (d) top.

It can be seen from the simulation results that the antenna has good directivity and matching characteristic with the human head medium. The electromagnetic waves emitted by the antenna can be effectively transmitted in the human head and meet the safety standards.

5. CONCLUSION

This research designs a new type of RBR with a wide reflection bandwidth, high reflectivity, and reflection frequency band of 2.61 GHz to 5.59 GHz (72.68%). The reflector is loaded to an elliptical monopole antenna. The antenna has the advantages of directional radiation, low profile (profile height of 0.12λ), and wide frequency band. The measured impedance bandwidth is 2.12 GHz to 6 GHz (95.57%). The front-to-back ratio bandwidth (FBR > 10 dB) is 2.2 GHz to 4.68 GHz (72.09%). The antenna is also a good choice for bio-electromagnetic applications.

ACKNOWLEDGMENT

This work was supported in part by National Natural Science Foundation of China under Grant No. 61661011, in part by China Postdoctoral Science Foundation under Grant No. 2019M653371, and in part by Key Laboratory of Cognitive Radio and Information Processing, Ministry of Education (Guilin University of Electronic Technology) under Grant No. CRKL190101.

REFERENCES

1. Lestari, A. A., A. G. Yarovoy, and L. P. Ligthart, "Adaptive wire bow-tie antenna for GPR applications," *IEEE Transactions on Antennas & Propagation*, Vol. 53, No. 5, 1745–1754, 2005.
2. Bashri, M. S. R., T. Arslan, and W. Zhou, "A compact RF switching system for wearable microwave imaging," *Antennas & Propagation Conference*, 1–4, 2016.
3. Krauns, J. D. and R. J. Marhefka, *Antennas: For All Applications*, 4rd Edition, 2002.
4. Jam, S. and M. Simruni, "Performance enhancement of a compact wideband patch antenna array using EBG structures," *AEU — International Journal of Electronics and Communications*, Vol. 89, 42–55, 2018.
5. Cheng, H., J. Chen, and X. Y. Wu, "Combining FSS and EBG surfaces for high-efficiency transmission and low-scattering properties," *IEEE Transactions on Antennas & Propagation*, Vol. 66, No. 3, 1628–1632, 2018.
6. Cao, Y. F. and X. Y. Zhang, "A wideband beam-steerable slot antenna using artificial magnetic conductors with simple structure," *IEEE Transactions on Antennas and Propagation*, Vol. 66, No. 4, 1685–1694, 2018.
7. Cao, Y. F., X. Y. Zhang, and T. Mo, "Low-profile conical-pattern slot antenna with wideband performance using artificial magnetic conductors," *IEEE Transactions on Antennas and Propagation*, Vol. 66, No. 5, 2210–2218, 2018.
8. Sievenpiper, D., L. Zhang, R. F. J. Broas, N. G. Alexopolous, and E. Yablonovitch, "High-impedance electromagnetic surfaces with a forbidden frequency band," *IEEE Transactions on Microwave Theory and Techniques*, Vol. 47, No. 11, 2059–2074, 1999.
9. Ranga, Y., L. Matekovits, K. P. Esselle, and A. R. Weily, "Multioctave frequency selective surface reflector for ultrawideband antennas," *IEEE Antennas and Wireless Propagation Letters*, Vol. 10, 219–222, 2011.
10. Peng, L., J. Y. Xie, and K. Sun, "Resonance-based reflector and its application in unidirectional antenna with low-profile and broadband characteristics for wireless applications," *Sensors*, Vol. 16, No. 12, 2092, 2016.
11. Peng, L., J. Y. Xie, and X. F. Li, "Front to back ratio bandwidth enhancement of resonance based reflector antenna by using a ring-shape director and its time-domain analysis," *IEEE Access*, Vol. 5, 15318–15325, 2017.

12. Xie, J. Y., L. Peng, and B. J. Wen, “Archimedean spiral antenna with two opposite unidirectional circularly polarized radiation bands designed by resonance based reflectors,” *Progress In Electromagnetics Research Letters*, Vol. 70, 23–30, 2017.
13. Wen, B. J., L. Peng, and X. F. Li, “A low-profile and wideband unidirectional antenna using bandwidth enhanced resonance-based reflector for fifth generation (5G) systems applications,” *IEEE Access*, Vol. 7, 27352–2736, 2019.